

Cooperative Reactivity of Early–Late Heterodinuclear Transition Metal Complexes with Polar Organic Substrates

Lutz H. Gade,^{*,[a]} Harald Memmler,^[a] Uta Kauper,^[a] Andreas Schneider,^[a] Sylvie Fabre,^[a] Izoldi Bezougli,^[a] Matthias Lutz,^[a] Christian Galka,^[a] Ian J. Scowen,^[b] and Mary McPartlin^[b]

Dedicated to Professor Jean-Marie Lehn on the occasion of his 60th birthday

Abstract: A comprehensive investigation into the cooperative reactivity of two chemically complementary metal-complex fragments in early–late heterodinuclear complexes has been carried out. Reaction of the partially fluorinated tripodal amidozirconium complexes $[\text{HC}\{\text{SiMe}_2\text{NR}\}_3\text{Zr}(\mu\text{-Cl})_2\text{Li}(\text{OEt}_2)_2]$ ($\text{R} = 2\text{-FC}_6\text{H}_4$: **2a**, $2,3,4\text{-F}_3\text{C}_6\text{H}_4$: **2b**) with $\text{K}[\text{CpM}(\text{CO})_2]$ ($\text{M} = \text{Fe}, \text{Ru}$) afforded the stable metal–metal bonded heterodinuclear complexes $[\text{HC}\{\text{SiMe}_2\text{NR}\}_3\text{-Zr-MCp}(\text{CO})_2]$ (**3–6**). Reaction of the dinuclear complexes with methyl isonitrile as well as the heteroallenes CO_2 , CS_2 , RNCO and RNCS led to insertion into the polar metal–metal bond. Two of these complexes, $[\text{HC}\{\text{SiMe}_2\text{N}(2\text{-FC}_6\text{H}_4)\}_3\text{Zr}(\text{S}_2\text{C})\text{Fe}(\text{CO})_2\text{Cp}]$ (**9a**) and $[\text{HC}\{\text{SiMe}_2\text{N}(2\text{-FC}_2\text{H}_4)\}_3\text{Zr}(\text{SCNPh})\text{Fe}(\text{CO})_2\text{-Cp}]$ (**12**), have been structurally characterized by a single crystal X-ray structure analysis, proving the structural situation of the inserted substrate as a bridging ligand between the early and late transition metal centre. The reactivity towards organic carbonyl deriva-

tives proved to be varied. Reaction of the heterobimetallic complexes with benzyl and ethylbenzoate led to the cleavage of the ester generating the respective alkoxozirconium complexes $[\text{HC}\{\text{SiMe}_2\text{N}(2\text{-FC}_6\text{H}_4)\}_3\text{ZrOR}]$ ($\text{R} = \text{Ph-CH}_2$: **13a**, Et : **13b**) along with $[\text{CpFe}\{\text{C}(\text{O})\text{Ph}\}(\text{CO})_2]$, whereas the analogous reaction with ethyl formate gave **13b** along with $[\text{CpFeH}(\text{CO})_2]$; this latter complex results from the instability of the formyliron species initially formed. Aryl aldehydes were found to react with the Zr-M complexes according to a Cannizzaro disproportionation pattern yielding the aroyliron and ruthenium complexes along with the respective benzyloxozirconium species. The transfer of the aldehyde hydrogen atom in the course of the reaction was established in a deuteration experiment. $[\text{HC}\{\text{SiMe}_2\text{-}$

$\text{N}(2\text{-FC}_6\text{H}_4)\}_3\text{Zr-M}(\text{CO})_2\text{Cp}]$ reacted with lactones to give the ring-opened species containing an alkoxozirconium and an acyliron or acylruthenium fragment; the latter binds to the early transition metal centre through the acyl oxygen atom, as evidenced from the unusually low-field shifted ^{13}C NMR resonances of the $\text{RC}(\text{O})\text{M}$ units. Ketones containing $\alpha\text{-CH}$ units react with the Zr-Fe complexes cooperatively to yield the aldol coupling products coordinated to the zirconium complex fragment along with the hydridoiron compound $[\text{CpFeH}(\text{CO})_2]$, whereas 1,2-diphenylcyclopropanone underwent an oxygen transfer from the keto group to a CO ligand to give a linking CO_2 unit and a cyclopropenylidene ligand coordinated to the iron fragment in $[\text{HC}\{\text{Si}(\text{CH}_3)_2\text{N}(2,3,4\text{-F}_3\text{C}_6\text{H}_2)\}_3\text{Zr}(\mu\text{-O}_2\text{C})\text{-Fe}(\text{CO})\{\text{C}_3\text{Ph}_2\}\text{Cp}]$ (**19**). The atom transfer was established by ^{17}O and ^{13}C labelling studies. Similar oxygen-transfer processes were observed in the reactions with pyridine N -oxide, dimethylsulfoxide and methylphenylsulfoxide.

Keywords: aldol reactions • Cannizzaro reactions • metal–metal interactions • oxygen-transfer reactions • transition metals

Introduction

Early–late heterodinuclear complexes in which the two metal centres are fixed at close proximity to each other have been studied with the aim of establishing cooperative reactivity

[a] Prof. L. H. Gade, Dr. H. Memmler, U. Kauper, A. Schneider, Dr. S. Fabre, Dr. I. Bezougli, M. Lutz, C. Galka
Laboratoire de Chimie Organométallique et de Catalyse
Institut Le Bel, Université Louis Pasteur
4, rue Blaise Pascal, 67070 Strasbourg Cedex (France)
E-mail: gade@chimie.u-strasbg.fr

[b] Dr. I. J. Scowen, Prof. M. McPartlin
School of Applied Chemistry, University of North London
Holloway Road, London N7 8DB (UK)

between the electronically very different reactive sites.^[1–3] In particular, dinuclear complexes in which the two metal atoms are directly bonded to each other may display this pattern of reactivity upon cleavage of the metal–metal bond and interaction of the substrate with the two complex fragments.^[4] In this case, the metal–metal bond “masks” the two coordinatively and electronically unsaturated complex fragments, which are liberated upon its dissociation. In the simplest case such heterodinuclear complexes will react as pairs of metal electrophiles and nucleophiles. Cooperative reactivity is thus particularly likely with polar substrates. In this case the electropositive early transition metal centre may react with the more Lewis basic part of the substrate, while the

nucleophilic late transition metal complex fragment will attack the more Lewis acidic part of the substrate molecule.^[5] In many cases it is difficult to establish whether the cleavage of the metal–metal bond precedes the transformation of the substrate or whether it occurs at a later stage. At least for simple transformations it was hoped to gain insight into the early reaction steps in the interaction of the substrate with the complex.^[6]

We have previously established a series of early–late heterobimetallic complexes which contain unsupported, highly polar metal–metal bonds.^[7–9] In particular, the use of tripodal amido ligands for the stabilization of the early transition metal centre has resulted in systems of unprecedented stability.^[7, 8] Apart from the kinetic stabilization due to steric shielding of the metal–metal bond by the ligand periphery, the coordination of the amido tripod to a high-valent metal generates a fairly rigid cage structure, in which the geometry of the early transition metal complex fragment is fixed in such a way that geometric “relaxation” upon cleavage of the metal–metal bond is suppressed. This situation is responsible for an additional thermodynamic stabilization of the dinuclear compounds.^[10]

Some preliminary studies into their reactive behaviour have been carried out indicating the general pattern described above.^[11, 12] In this paper we give a comprehensive account of the reactive behaviour of such heterodinuclear complexes towards a wide variety of organic substrates most of which contain unsaturated functional groups. The assumptions related to the cooperative reactive potential of the complementary metal complex fragments—frequently raised in the past—were thus put to an experimental test. To this end, it proved necessary to employ amido ligand systems that contain partially fluorinated aryl groups as peripheral *N*-substituents. These were found to confer the additional stability upon the molecules necessary for their systematic investigation.

Results and Discussion

Synthesis of the heterodinuclear complexes stabilised by partially fluorinated tripodal amido ligands: We previously found that the key to success in the stabilization of unsupported early–late heterodinuclear complexes is the appropriate choice of the ligand system in the early transition metal complex fragment. Of the tripodal amido ligands studied by us, those containing peripheral *N*-bound 2-fluorophenyl groups were found to confer greatest stability upon these systems.^[13, 14] Whether this is due to the influence which the substituents have on the electronic properties of the amido *N*-donor functions or a consequence of the participation of the fluorophenyl groups in the coordination to the metal cannot be generally distinguished. In the heterodinuclear complexes described in this work the previously reported ligand system derived from $\text{HC}\{\text{SiMe}_2\text{N}(2\text{-FC}_6\text{H}_4)\}_3$ (**1a**)^[13] has been employed as well as the novel trifluorinated compound $\text{HC}\{\text{SiMe}_2\text{N}(2,3,4\text{-F}_3\text{C}_6\text{H}_2)\}_3$ (**1b**), which was synthesized by an analogous route. Stabilization of early transition metal amido complexes by fluorinated aryl substituents has also been reported by Schrock and co-workers, who synthesized a series

of pentafluorophenyl-substituted amido compounds.¹⁵ However, the completely fluorinated analogue of **1a** and **1b** is not accessible by the established synthetic route for this type of ligand.

The starting materials for the Zr–Fe and Zr–Ru heterodinuclear complexes were the chlorozirconium complexes $[\text{HC}\{\text{SiMe}_2\text{NR}\}_3\text{Zr}(\mu\text{-Cl})_2\text{Li}(\text{OEt}_2)_2]$ ($\text{R} = 2\text{-FC}_6\text{H}_4$: **2a**, 2,3,4- $\text{F}_3\text{C}_6\text{H}_2$: **2b**). Whereas the identity and structure of compound **2a** was established in an earlier study,^[13] the more highly fluorinated complex **2b** was structurally characterized in this study in order to compare the role which the peripheral fluorine atoms play in both compounds. Its molecular structure is displayed in Figure 1; the principal bond lengths and angles are given in the legend.

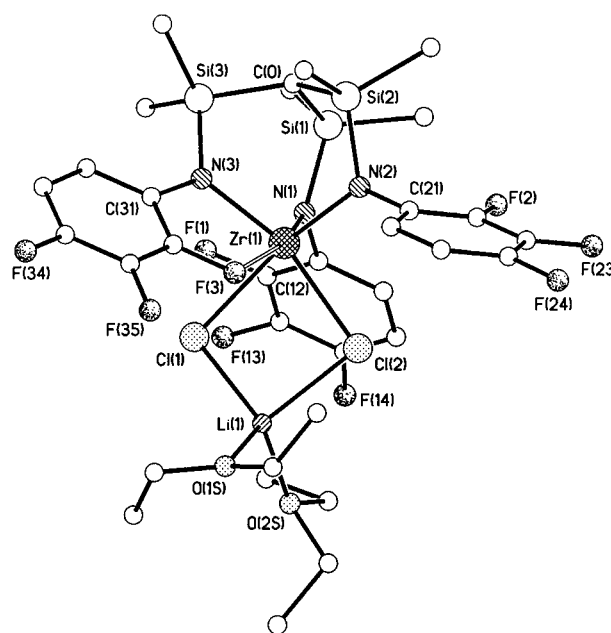
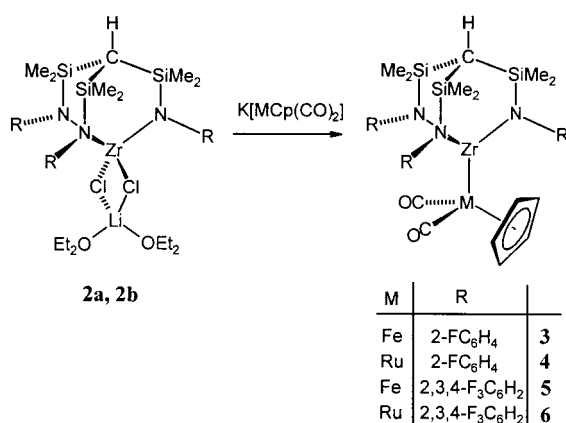


Figure 1. Molecular structure of the chlorozirconium complex **2b**. Principal bond lengths [Å] and angles [°]: Zr(1)–Cl(1) 2.575(2), Zr(1)–Cl(2) 2.592(2), Li(1)–Cl(1) 2.328(19), Li(1)–Cl(2) 2.351(19), Cl(1)–Zr(1)–Cl(2) 81.73(8), Cl(1)–Zr(1)–Cl(2) 91.1(6), O(1S)–Li(1)–O(2S) 107.3(9).

As in the monofluorophenyl analogue **2a**, the coordination at the central zirconium atom may be described as highly distorted octahedral with three amido-nitrogen atoms in facial sites [Zr–N 2.052(6)–2.119(6) Å], two bridging chloro ligands [Zr–Cl(1) 2.575(2) and Zr–Cl(2) 2.529(2) Å] and with the sixth site being occupied by the *ortho*-fluorine atom of one of the phenyl groups. The Zr⋯F(3) bond length of 2.647(5) Å is slightly longer than the corresponding bond length of 2.535(5) Å observed in **2a** and that of 2.511(2) Å in the related compound $[\text{MeSi}\{\text{SiMe}_2\text{N}(2\text{-FC}_6\text{H}_4)\}_3\text{Zr}(\mu\text{-Cl})_2\text{Li}(\text{OEt}_2)_2]$;^[13, 14, 16] however, considerable bonding character is indicated by the extent to which the phenyl ring is forced over to allow this chelate ring formation, giving a N(3)–C(31)–C(36) intra-chelate angle of 114.6(4)° compared with 125.3(4)° for N(3)–C(31)–C(32).

Upon reaction of **2a** and **2b** with $\text{K}[\text{MCp}(\text{CO})_2]$ in toluene, the heterobimetallic complexes $[\text{HC}\{\text{SiMe}_2\text{NR}\}_3\text{Zr-MCp}(\text{CO})_2]$ (**3–6**) are formed (Scheme 1), which may be isolated

Scheme 1. Synthesis of the heterobimetallic complexes **3**–**6**.

directly from the reaction mixture as yellow microcrystalline solids. The resonance pattern in the ¹H, ¹³C, ²⁹Si and ¹⁹F NMR spectra recorded at 295 K are consistent with an effective local C_{3v} symmetry of the amidozirconium fragment; this indicates rapid internal rotation around the Zr–M bonds in these molecules. The formation of the metal–metal bond is typically reflected in the considerable shift of the ν(CO) bands to higher wavenumbers relative to the alkali metal carbonoylates (Table 1).^[7, 8] The formation of the dinuclear compounds occurs sufficiently selectively to allow their in situ generation in some of the reactions described below.

Table 1. Infrared carbonyl stretching frequencies of the Zr–M heterodinuclear complexes reported in this work.

	ν(CO) (ν _{sym} , ν _{as}) [cm ⁻¹]
Zr–Fe	
K[FeCp(CO) ₂] ^[a]	1866, 1772
3	1972, 1917
5	1976, 1921
Zr–Ru	
K[RuCp(CO) ₂] ^[a]	1896, 1811
4	1992, 1936
6	1985, 1925

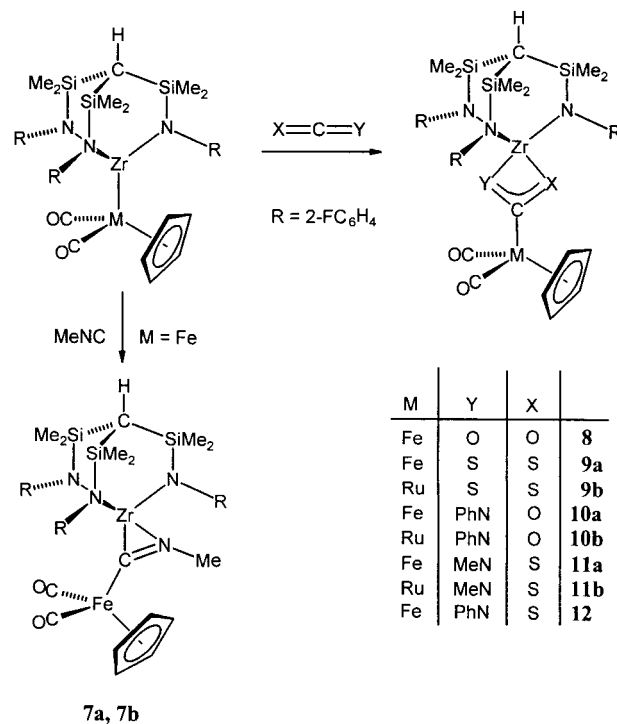
[a] Data from ref. [25].

Insertion of unsaturated polar substrates into the metal–metal bonds:

The simplest pattern of reactivity observed for the Zr–M heterodinuclear compounds is the insertion of an unsaturated polar substrate into the metal–metal bonds. The first such reaction was reported in a study by Culter and co-workers,^[17] who showed that Casey's Zr–M heterobimetallic complexes insert CO₂ into their metal–metal bond, while Bergman et al. studied the reactions of an imido-bridged Ir–Zr complex with CO₂, CS₂ and MeNCS, the last two undergoing fragmentation in the course of the reaction.^[18] We have previously reported the insertion of isonitriles into the polar metal–metal bond of early–late heterobimetallic complexes that are related to those reported in this paper.^[8] Reaction of **3** and **6** with methyl isonitrile leads to similar types of products, [HC(SiMe₂N(2-FC₆H₄))₃Zr(η²-C(=NMe)-FeCp(CO)₂)] (**7a**) and [HC(SiMe₂N(2,3,4-F₃C₆H₂))₃Zr(η²-C(=NMe)RuCp(CO)₂)] (**7b**) (see Scheme 3 later). However, these are thermally unstable and could only be characterized

NMR spectroscopically in solution below 260 K. The characteristic ¹³C NMR chemical shift of the resonance attributable to the carbon atom inserted between the two metals (**7a**: δ = 280.8; **7b**: δ = 275.9), and the clean set of resonances attributable to the relevant molecular fragments indicate its selective formation.

More stable insertion products were obtained in the reactions of **3** and **4** with X=C=Y heteroallenes. Reaction of these Zr–M complexes with one molar equivalent of CO₂, CS₂, phenyl isocyanate, phenyl isothiocyanate or methyl isothiocyanate yielded the insertion products **8**–**12** shown in Scheme 2. The formulations and structural proposals of the

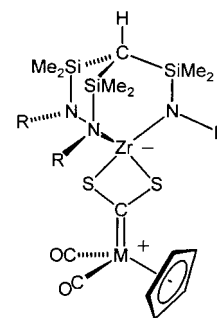


Scheme 2. Insertion of polar unsaturated organic substrates into the polar metal–metal bonds.

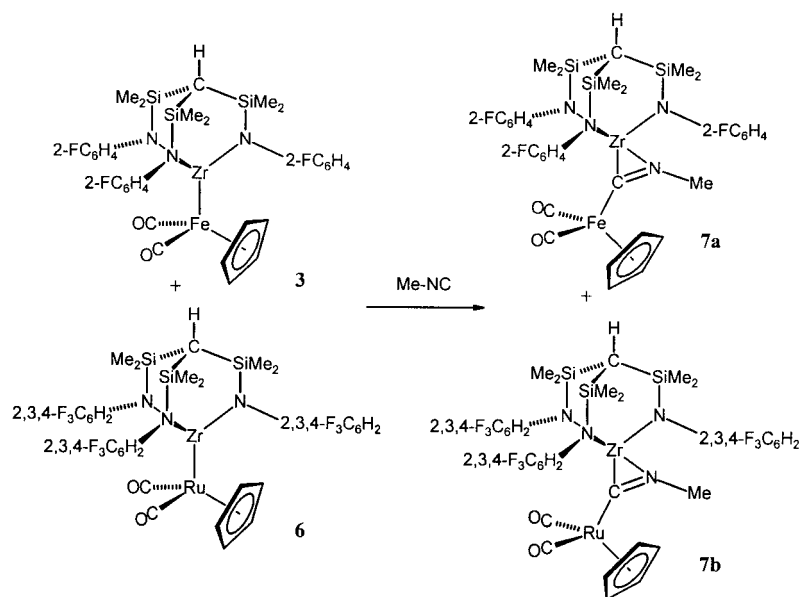
reaction products are supported by the analytical data as well as the ¹H, ¹³C, ²⁹Si, ¹⁹F NMR and infrared spectroscopic data.

Their most remarkable spectroscopic feature is the ¹³C NMR shift of the heteroallene carbon resonances [δ (¹³C) **8** 240.7, **9a** 334.0, **9b** 320.6, **10a** 236.1, **10b** 221.0, **11a** 241.4, **11b** 226.5, **12** 248.9]. Of these the position of the signal attributable to the ¹³CS₂ carbon in **9a** and **9b** is observed at remarkably low field (δ = 334.0 and 320.6, respectively), a situation which indicates a partial carbenoid character of the inserted carbon disulfide (best represented by a zwitterionic resonance structure of the dinuclear complex with the negative charge at Zr and the positive charge at M).

Of principal mechanistic interest is the question whether the interaction of the two com-



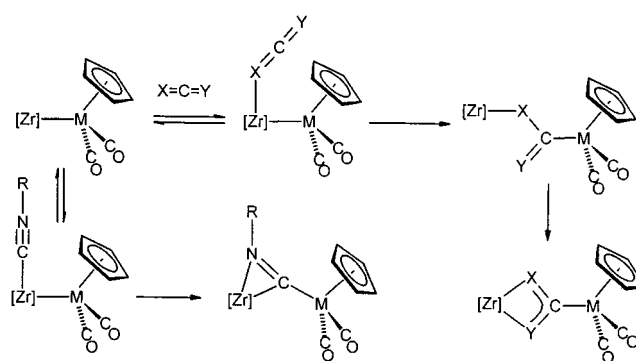
plex fragments with the substrates occurs separately, that is, after dissociation in solution, or cooperatively. The fact that no significant enhancement—but rather a decrease—of the reaction rate of the insertion of MeNCS is observed when the reaction is carried out and monitored by ^{19}F NMR spectroscopy in $[\text{D}_6]\text{THF}$ instead of $[\text{D}_8]\text{toluene}$ supports the notion that solvated ionic intermediates do not seem to determine the pathway of the conversion.^[11] Secondly, the significantly greater reaction rate of the oxygen-containing heteroallenes (CO_2 and PhNCO) and the absence of detectable intermediates suggests that the conversion is strongly influenced by the interaction of the donor atom in the substrate with the heterodinuclear complex. Moreover, the availability of two structurally related zirconium complex fragments and the two $\{\text{MCp}(\text{CO})\}$ units enabled us to carry out the crossover experiment depicted in Scheme 3.



Scheme 3. Cross-over experiment of the insertion of methyl isocyanide into the metal–metal bonds of complexes **3** and **6**. No cross-over products indicating the exchange of complex fragments were detected.

Reaction of a mixture of equimolar amounts of $[\text{HC}(\text{SiMe}_2\text{N}(2\text{-FC}_6\text{H}_4))_3\text{Zr-FeCp}(\text{CO})_2]$ (**3**) and $[\text{HC}(\text{SiMe}_2\text{N}(2,3,4\text{-F}_3\text{C}_6\text{H}_2))_3\text{Zr-RuCp}(\text{CO})_2]$ (**6**) with MeNC at 260 K led exclusively to the complexes **7a** and **7b**. The absence of any crossover products implies that the interaction of both complex fragments with the substrate must occur within the solvent cage of the heterodinuclear complex. The combined evidence obtained in these studies has led us to propose the mechanism for the insertion reaction depicted in Scheme 4.

In a first step, the polar unsaturated substrate coordinates to the zirconium centre in a Lewis acid/base type interaction. This increase in the coordination number at the zirconium leads to a polarization and concomitant labilization of the metal–metal bond that is cleaved. This is followed by the insertion of the substrate between the two metal centres according to a pattern of complementary polarity [the nucleophilic late transition metal fragment attacking the electrophilic carbon atom of the substrate and the electro-



Scheme 4. Proposed mechanism for the insertion of isocyanides and heteroallenes into the polar metal–metal bonds.

negative donor function(s) of the substrate coordinating to the Zr centre]. We have recently shown that this type of reactivity strongly depends on the nucleophilic properties of the late transition metal fragment.^[6] In a related system, substitution of the Fe or Ru carbonyl complex units by the less nucleophilic $\{\text{Co}(\text{CO})_4\}$ fragment led exclusively to heterolytic (i.e., ionic) cleavage of the metal–metal bond. We have also shown that for certain substrates the insertion step may be reversible. This has been observed in the reaction of $[\text{MeSi}(\text{SiMe}_2\text{N}(p\text{-Tol}))_3\text{Zr-RuCp}(\text{CO})_2]$ with $t\text{BuNC}$.^[6] The latter does not insert into the metal–metal bonds of **3–6**, and it is only the absence of $^1J(^{14}\text{N},^{13}\text{C})$ coupling in the otherwise unchanged ^{13}C NMR spectrum of the isonitrile in the presence of **3–6** that indicates a weak and reversible interaction with the metal complex, most likely of the kind postulated in Scheme 4.

In order to determine the coordination mode of the XC_2Y ligand ($\text{X} = \text{O}, \text{S}; \text{Y} = \text{O}, \text{S}, \text{NR}$) to the early and late transition metal centres as a result of the insertion into the metal–metal bond, single-crystal X-ray structure analyses of **9a** and **12** were carried out. Despite relatively weak diffraction from the available samples the principal structural features of both **9a** and **12** were clearly established (Figure 2).

Although there was considerable disorder of the tripodal ligand framework in the crystal of **12** it is clear that the overall coordination of the zirconium atom in both **9a** and **12** bears a striking resemblance to that found in the dichloride **2b** (vide supra) and in the dichloro starting material **2a**. As in the dichlorides, the tripodal ligands in the insertion products **9a** and **12** both effectively occupy *four* coordination sites of the zirconium atom, with three facial nitrogen donors and an interaction from the *ortho*-fluoro atom of a peripheral phenyl ring at the fourth site (Table 2). The $\text{Zr}\cdots\text{F}(3)$ bond length of

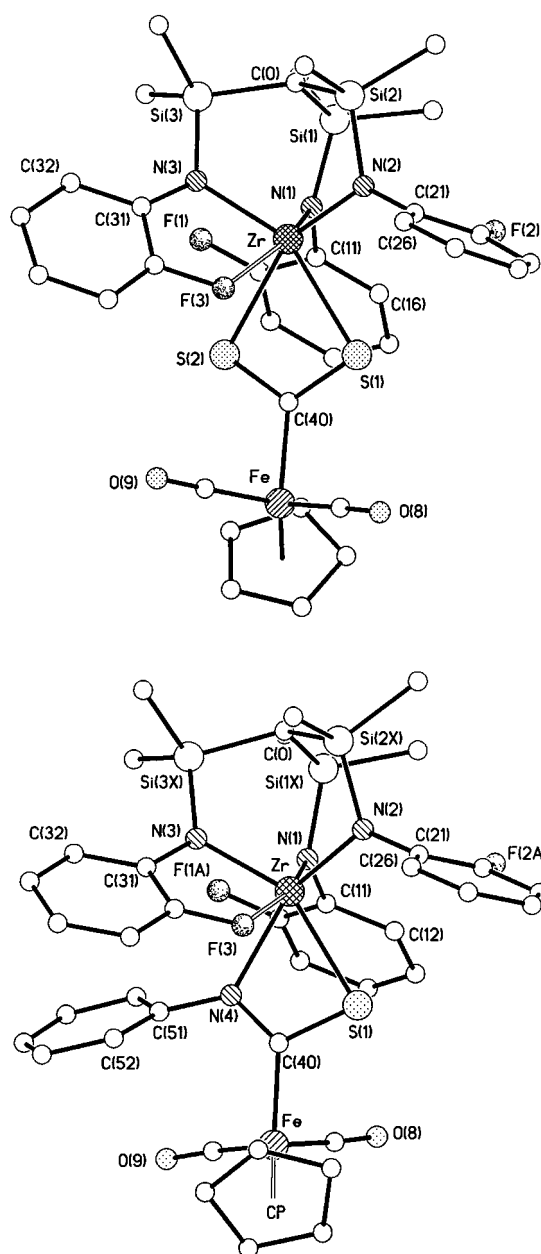


Figure 2. Top: molecular structure of the CS₂ insertion product **9a**. Principal bond lengths [Å] and angles [°]: Zr–S(1) 2.632(4), Zr–S(2) 2.643(3), S(1)–C(40) 1.717(10), S(2)–C(40) 1.708(10), Fe–C(40) 1.934(11), Fe–C(8) 1.773(12), Fe–C(9) 1.785(11), S(1)–Zr–S(2) 66.88(10), C(8)–Fe–C(9) 94.2(6), S(1)–C(40)–S(2) 116.1(7); Bottom: molecular structure of the PhNCS insertion product **12**. Principal bond lengths [Å] and angles [°]: Zr–S(1) 2.571(5), Zr–N(4) 2.282(13), C(40)–N(4) 1.307(22), C(40)–S(1) 1.745(17), Fe–C(40) 1.952(17), N(4)–Zr–S(1) 62.7(3), C(8)–Fe–C(9) 87(1), N(4)–C(40)–S(1) 112(1).

2.560(7) Å in **9a** is very similar to that of 2.535(5) Å previously found in the dichloro starting material **2a**,^[13] and although in **12** this distance is rather longer [Zr⋯F(3) 2.70(1) Å], being closer to that in **2b** [2.647 Å], the interaction appears bonding in both insertion compounds. As in **2b** (vide supra), the coordinating fluorophenyl ring is apparently being forced over to facilitate chelation [N(3)–C(31)–C(32) 125.1(8) and 124(1)°, and N(3)–C(31)–C(36) 114.8(8) and 116(1)° in **9a** and **12**, respectively]. In both dichlorides, and

Table 2. Comparison of selected bond lengths [Å] and angles [°] for the tripodal ligand coordination in **2b**, **9a**, **12** and the previously reported structure **2a**.

	2a ^[a]	2b	9a	12
Zr–N(1)	2.040(7)	2.052(6)	2.060(8)	2.053(12)
Zr–N(2)	2.072(7)	2.084(6)	2.101(8)	2.093(13)
Zr–N(3)	2.125(6)	2.119(6)	2.124(8)	2.105(11)
Zr⋯F(3)	2.535(5)	2.647(5)	2.554(7)	2.703(11)
Si(1)–N(1)	1.755(7)	1.768(7)	1.734(8)	1.753(14)
Si(2)–N(2)	1.740(7)	1.773(6)	1.756(9)	1.742(14)
Si(3)–N(3)	1.741(7)	1.769(6)	1.758(8)	1.763(12)
N(1)–C(11)	1.43(1)	1.420(7)	1.449(9)	1.41(2)
N(2)–C(21)	1.44(1)	1.420(7)	1.435(10)	1.43(2)
N(3)–C(31)	1.39(1)	1.416(7)	1.422(9)	1.43(2)
N(1)–Zr–N(2)	98.4(3)	100.4(2)	102.9(3)	100.4(5)
N(1)–Zr–N(3)	101.8(3)	102.7(2)	103.7(3)	103.3(5)
N(2)–Zr–N(3)	95.1(3)	95.7(2)	101.7(3)	100.0(5)
Zr–N(1)–Si(1)	117.4(4)	116.2(3)	114.5(4)	114.2(7)
Zr–N(2)–Si(2)	115.2(3)	113.2(3)	110.1(5)	111.6(6)
Zr–N(3)–Si(3)	116.1(3)	114.3(3)	111.6(4)	112.9(6)
Zr–N(1)–C(11)	124.5(6)	122.3(5)	121.7(6)	125.3(9)
Zr–N(2)–C(21)	128.1(6)	128.9(4)	130.4(7)	126.2(9)
Zr–N(3)–C(31)	120.5(6)	123.6(4)	123.6(6)	122.3(8)
Zr–F(3)–C(36)	108.7(5)	106.5(3)	109.7(6)	105.7(8)
Si(1)–N(1)–C(11)	116.0(6)	119.1(3)	123.3(7)	118(1)
Si(2)–N(2)–C(21)	115.9(6)	116.5(4)	118.7(6)	121(1)
Si(3)–N(3)–C(31)	123.4(6)	122.1(4)	124.8(7)	125(1)

[a] Re-numbered from ref. [13].

in the insertion product **9a**, the zirconium–nitrogen bond within the five membered chelate ring is the longest [Zr–N(3): 2.125 (**2a**), 2.119(6) (**2b**) and 2.124(8) Å (**9a**)] and that *trans* to the coordinating fluorine atom is the shortest [Zr–N(1): 2.040(7) (**2a**), 2.056(6) (**2b**) and 2.060(8) (**9a**)]. The shortening of the Zr–N(1) bond in each of these compounds is consistent with enhanced π donation from the amide donor *trans* to the highly electronegative fluoro atom. Although these trends also appear to be present in **12**, the relatively high esd's caused by the extensive disorder of the tripod mean that the differences are of low significance. The persistence of the fluoro–zirconium interaction, from its presence in the starting material **2a** to that in the heterodinuclear insertion products **9a** and **12**, demonstrates the importance of the “active” ligand periphery in these compounds.

The central structural unit in **9a** is the bent CS₂ fragment [S(1)–C(41)–S(2) 116.1(7)°] that links the two metal centres. Both of the S atoms bond directly to the zirconium [Zr–S(1) 2.632(4), Zr–S(2) 2.643(3) Å]. The NCS heteroallene, linear in the free isothiocyanate, is bent in **12** [N(4)–C(2)–S(1) 112(1)°] and bridges the metals in a manner similar to that found in the CS₂ analogue **9a**. Whereas the C–S bond length of 1.745(17) Å lies in the range of a C–S single bond, the carbon–nitrogen bond [1.307(22) Å] retains considerable double bond character.^[19]

Reactions of the heterodinuclear complexes with esters and aldehydes: The reactions described in the previous section lead to stable products of insertions into the polar metal–metal bond. Substrates, such as carboxylic esters, which have predetermined points of cleavage in their molecular structure or, such as aldehydes and ketones, offer alternative reaction

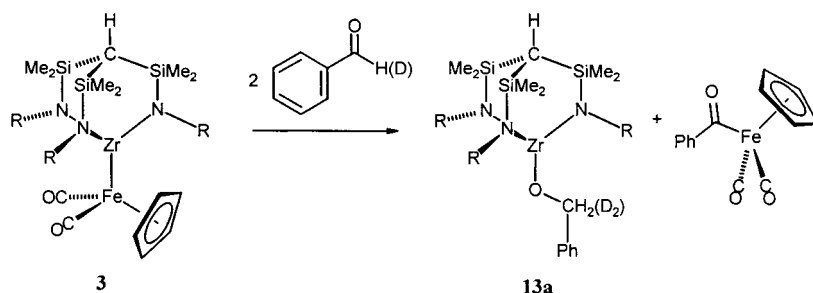
pathways may undergo further conversions as will be discussed in this and the next section.

Reaction of the Zr–Fe complex **3** with one molar equivalent of PhC(O)OR (R = Et, CH₂Ph) immediately leads to the cleavage of the ester to give a 1:1 mixture of the alkoxyzirconium complex [HC{SiMe₂N(2-FC₆H₄)₃Zr-OR] (R = CH₂Ph: **13a**, Et: **13b**) and the known benzoyliron complex [FeCp{C(O)Ph}(CO)₂] (Scheme 5). The identity of the compounds, which could not be completely separated, was confirmed by comparison with the data obtained of authentic samples, which were synthesized by an independent method. Whereas the iron complex is a known compound,^[20] **13a** and **13b** were prepared by reaction of **2a** with one molar equivalent of the respective lithium alkoxide.

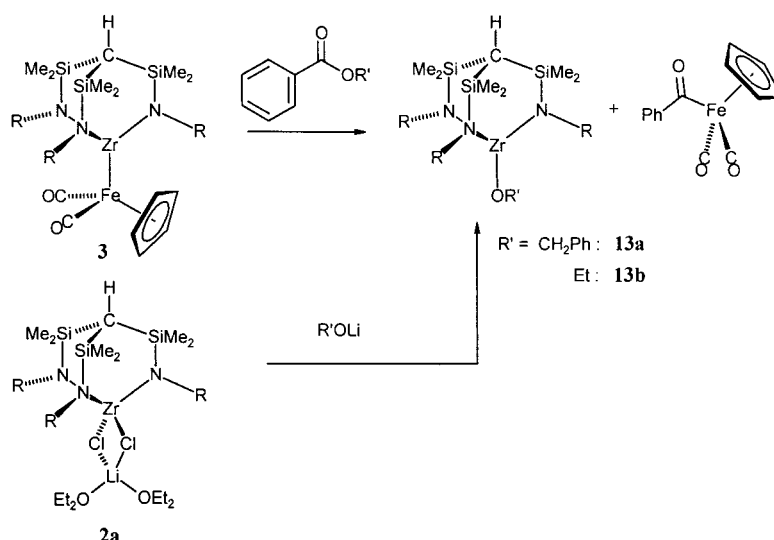
A similar reactive pattern is thought to be obtained even if the acyl metal fragment is unstable and therefore may not be detected. Upon reaction of **3** with ethylformate, immediate formation of **13a** and [CpFeH(CO)₂] is observed and infrared spectroscopy indicates the presence of uncoordinated CO ($\bar{\nu}$ = 2144 cm⁻¹). This is a consequence of the well-known instability of the formyl complex, which readily extrudes CO to form the hydrido species.

The generation of complex **13a** and the benzoyliron compound [FeCp{C(O)Ph}(CO)₂] is also observed in the reaction of **3** with two molar equivalents of benzaldehyde. Upon carrying out this reaction in an NMR tube by slowly adding the aldehyde to a solution of the Zr–Fe complex in [D₈]toluene, the stoichiometry could be established unambiguously. After addition of one equivalent of benzaldehyde only half of the Zr–Fe complex was converted to the products, which were identified by comparison of the spectroscopic data with those of a 1:1 sample mixture synthesized by the independent route mentioned above (Scheme 6).

Moreover, from the series of NMR spectra the absence of a detectible intermediate was established, which indicates their short lived nature. Formally, the reaction products are those of a Cannizzaro type disproportionation of an arylaldehyde.^[21]



Scheme 6. Cannizzaro type disproportionation of benzaldehyde and deuteriobenzaldehyde in the coordination spheres of the two complementary metal centres.



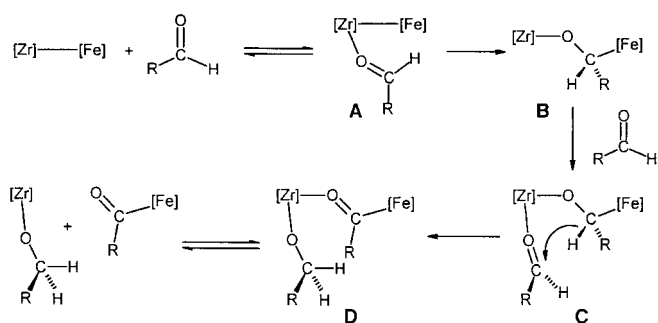
Scheme 5. Cleavage of benzoic acid esters to give the benzoyliron complex and the alkoxyzirconium product.

To establish the validity of this designation, the reaction was carried out with deuteriated benzaldehyde C₆H₅CDO.^[22] The ¹H NMR spectrum of the reaction products displays the identical set of resonances as that in the experiments with the unlabelled compounds with the exception of the benzyl-CH₂ signal at δ = 4.66, which is completely absent. That the hydrogen atom transfer only occurred between the benzylic positions and does not involve other H atoms was additionally confirmed by the presence of only one signal in the ²H NMR (δ = 4.6) spectrum assigned to the CD₂ group.

Similar experiments carried out in NMR tubes in [D₈]toluene at temperatures below –40 °C with benzaldehyde derivatives substituted in the *para* position, with the aim of detecting reaction intermediates, did not reveal resonance sets other than those of the starting materials and the products generated after successive addition of the aldehyde.^[23] This is testimony to the extreme rapidity of the hydrogen-atom transfer. However, in view of the result of the deuteration experiment we propose the reaction mechanism displayed in Scheme 7.

The first step in the reaction sequence is thought to be the addition of an aldehyde molecule to the Lewis acidic early transition metal centre, which is followed by its insertion into the metal–metal bond. The cleavage of the Zr–Fe bond reduces the coordination number at zirconium, which in turn facilitates the addition of the second molecule of benzaldehyde. The crucial reaction step is the hydride-transfer step, which follows and involves an analogous intermediate as that proposed for the Cannizzaro or Tishchenkov disproportionations.^[21] This gives the reaction products through the association equilibrium of **13a** and the benzoyliron complex.

Both the cleavage of esters and the disproportionation of the arylaldehydes yield stoi-



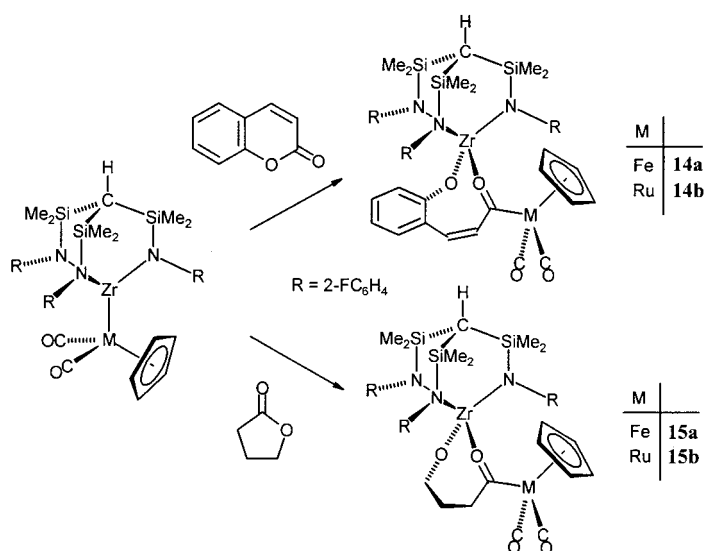
Scheme 7. Proposed mechanism for the hydride transfer in the arylaldehyde disproportionation reactions.

chiometric mixtures of two reaction products that are difficult to identify unambiguously unless these two components are accessible by independent synthetic routes. In order to avoid this complication the reactions of the Zr–Fe and Zr–Ru complexes **3** and **4** with the lactones cumarine and γ -butyrolactone were studied. In both cases selective lactone cleavage was observed to give the reaction products $[\text{HC}\{\text{SiMe}_2\text{N}(2\text{-FC}_6\text{H}_4)\}_3\text{ZrOC}_6\text{H}_4\text{CH}=\text{CHC}(\text{O})\text{MCp}(\text{CO})_2]$ (M = Fe: **14a**, Ru: **14b**) and $[\text{HC}\{\text{SiMe}_2\text{N}(2\text{-FC}_6\text{H}_4)\}_3\text{ZrO}(\text{CH}_2)_3\text{C}(\text{O})\text{MCp}(\text{CO})_2]$ (M = Fe: **15a**, Ru: **15b**), respectively (Scheme 8).

The most remarkable spectroscopic feature of these complexes, which formally may be viewed as products of an insertion into the metal–metal bond, is the ^{13}C NMR chemical shift of the signal attributed to the metallaacyl carbon nuclei. For the iron complexes **14a** and **15a**, this resonance is observed at $\delta = 291.3$ and 291.5 , respectively, while the corresponding signals of the Ru analogues **14b** and **15b** are observed at $\delta = 271.6$ and 272.5 , respectively. These chemical shifts lie considerably outside the range normally observed for acylmetal complexes of this type (M = Fe: $\delta = \text{ca. } 250$, M = Ru: $\delta = \text{ca. } 230$)^[24, 25] and are more akin to the values found for carbene complexes.^[25, 26] We therefore propose an additional coordination of the acyl group to the zirconium centres through the carbonyl oxygen atoms as is indicated in Scheme 8. We previously formulated a similar *O*-coordination to the early transition metal atom in a study of the ring-opening reactions of axially prochiral biaryl lactones with heterodinuclear complexes, a notion also based on the unusual ^{13}C NMR chemical shift of the acyl carbon nuclei.^[12] In this case, these complexes were found to be unstable with respect to subsequent decarbonylation. Such a reactive behaviour was not observed for compounds **14a/b** and **15a/b**.

Reactions of the heterodinuclear complexes with ketones:

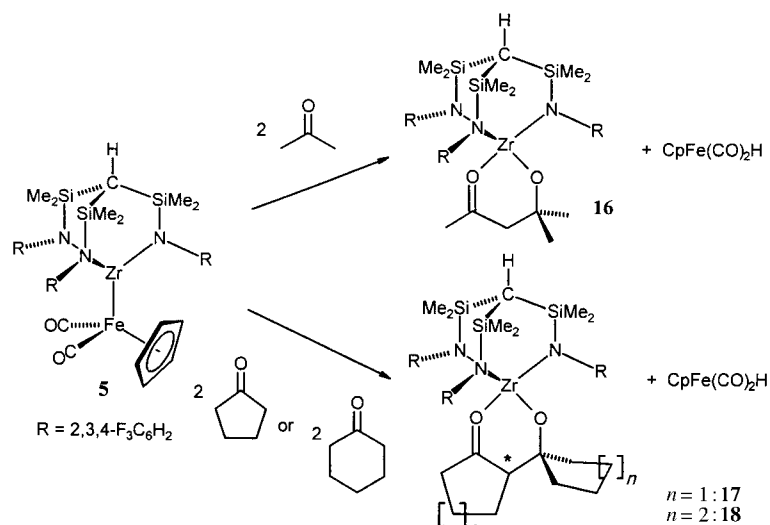
The reaction of the Zr–Fe di-



Scheme 8. Ring opening of lactones to give the metallaacyl complexes **14** and **15**.

nuclear complex **5** with ketones leads to immediate aldol coupling to give the corresponding zirconium complex, which contains the aldol product ligated to the Zr centre. Simultaneously, an equimolar amount of the hydridoiron complex $[\text{CpFe}(\text{CO})_2\text{H}]$ is formed.^[27] Upon addition of two molar equivalents of actone, cyclopentanone or cyclohexanone to compound **5** conversion occurs immediately to give the complexes **16**, **17** and **18**, respectively (Scheme 9).

Since attempts to isolate the pure products were hampered by their thermal lability and the difficulty of separating small amounts of $[\text{CpFe}(\text{CO})_2]_2$, which is generated via the hydridoiron half-sandwich complex, they were characterised by NMR spectroscopy. The signal patterns assigned to the coordinated tripodal ligand are consistent with a local threefold symmetry indicating dynamic exchange of the “turnstile” type that we have observed for all fivefold coordinate zirconium complexes to date. Whereas the aldol ligand in **16** is achiral, the newly formed organic units in **17**



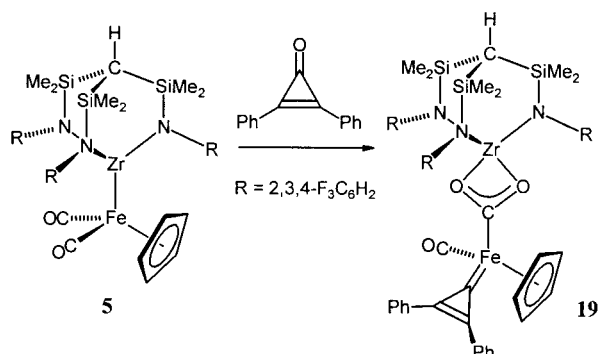
Scheme 9. Aldol coupling of ketones induced by Zr–Fe complex **5**.

and **18** each contain one chiral centre. This is reflected in the diastereotopic splitting of the ^1H and ^{13}C NMR resonances of the SiMe_2 groups and the chemical inequivalence of all the CH_2 proton and ^{13}C NMR signals of the two condensed carbocycles. The resonance of the quaternary C atom adjacent to the alkoxo-O atom at $\delta = 75.4, 88.5$ and 81.1 in the ^{13}C NMR spectra of **16**, **17**, and **18**, respectively, and the low-field chemical shift of the Zr-bonded carbonyl function (**16**: δ 225.3 **17**: 236.3, **18**: 231.2) are particularly characteristic for this type of metal coordinated aldol ligand.

The hydridoiron complex generated in these conversions is thought to be formed in a first reaction step following the insertion of the carbonyl group into the metal–metal bond. This yields an extremely reactive metal-bound enolate which in turn rapidly undergoes aldol coupling with a second molecule of ketone to give compounds **16–18**.

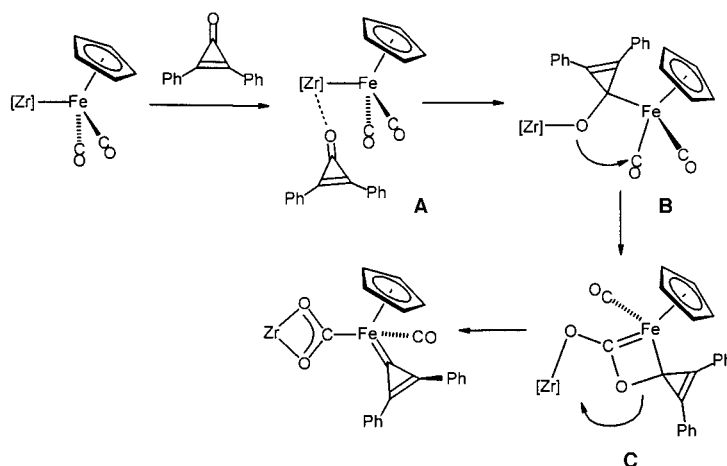
The aldol-type coupling reactions described above require the presence of α -CH protons in the substrates. In order to assess the reactivity of the heterodinuclear compounds towards ketones without α -protons we studied the reactions of complex **5** with benzophenone and 1,2-diphenylcyclopropanone. Whereas the former underwent an immediate redox-chemical process generating $[\text{CpFe}(\text{CO})_2]_2$ and a mixture of unidentifiable Zr-species, the reaction with 1,2-diphenylcyclopropanone proceeded cleanly to yield a single product, which was isolated as a yellow microcrystalline solid. The ^1H , ^{13}C and ^{29}Si NMR spectra are consistent with an effective threefold symmetry of the tripod-amidozirconium fragment, while the diastereotopic splitting of the SiMe_2 resonances in the ^1H and ^{13}C NMR spectra indicates the formation of a chiral centre at the late transition metal fragment. The infrared spectrum displays only a single $\nu(\text{CO})$ band at 1953 cm^{-1} establishing the presence of only one Fe-bonded carbonyl ligand. The ^{13}C carbonyl NMR resonance is observed at remarkably low field ($\delta = 219.3$); however, more importantly, two additional signals of equal intensity are found at even lower field, $\delta = 221.1$ and 259.0 . Moreover, the resonance of the carbonyl function in 1,2-diphenylcyclopropanone ($\delta = 156.4$) disappears and the signal of the C=C olefin unit in the cyclopropane ring is shifted from $\delta = 146.7$ to 179.5 . These data are consistent with a molecular structure of the reaction product $[\text{HC}\{\text{Si}(\text{CH}_3)_2\text{N}(2,3,4\text{-F}_3\text{C}_6\text{H}_2)\}_3\text{Zr}(\mu\text{-O}_2\text{C})\text{Fe}(\text{CO})\{\text{C}_3\text{Ph}_2\text{Cp}\}]$ (**19**) as shown in Scheme 10.

Similar to our previously reported deoxygenation of sulfoxides that yield reaction products which contain a $\mu\text{-CO}_2$



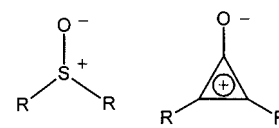
Scheme 10. Oxygen transfer from 1,2-diphenylcyclopropanone to an iron-bonded CO ligand in **5**.

ligand linking the early with the late transition metal centre,^[28] oxygen transfer from the cyclopropanone substrate to a carbonyl ligand has occurred to generate a $\mu\text{-CO}_2$ unit and an iron-bound carbene ligand, which is characterized by the ^{13}C NMR resonance at $\delta = 259.0$. The transformation of one of the CO ligands could be established by carrying out the reaction with a ^{13}C -enriched sample (10%) of **5** that yielded the labelled $\mu\text{-CO}_2$ unit, while the oxygen transfer was proved by reaction with 30% ^{17}O -enriched 1,2-diphenylcyclopropanone [$\delta(^{17}\text{O}) = 224$, reference dioxane].^[29] The chemical shift of the product signal of $\delta(^{17}\text{O}) = 365$ in the labelled complex **19** is indicative of an ^{17}O nucleus in a metallacarboxy environment.^[30] Attempts to study the kinetics of this reaction and thus gain additional insight concerning its mechanism were precluded by the extreme rapidity of the conversion and the air and moisture sensitivity of the compounds involved. However, given the results of the ^{13}C and ^{17}O labeling studies, we propose the reaction mechanism for this transformation displayed in Scheme 11.



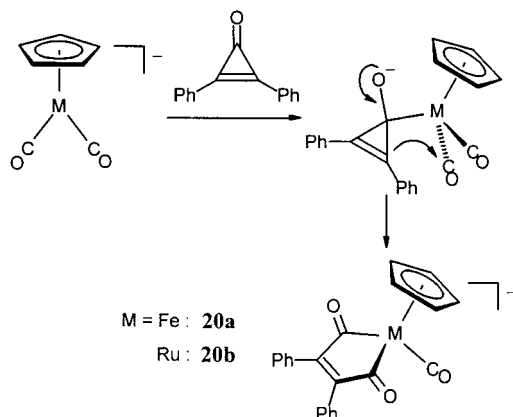
Scheme 11. Proposed mechanism for the deoxygenation of 1,2-diphenylcyclopropanone.

By analogy with the mechanism of the simple insertion reactions into the polar metal–metal bonds, the formation of a Lewis acid–base adduct (**A**) is thought to be the first step, in which the carbonyl group of the substrate is additionally polarized and the Zr–Fe bond labilized. The metal–metal bond is subsequently cleaved and the nucleophilic iron fragment attacks the electrophilic CO-carbon atom of the cyclopropanone to give intermediate **B**. Intramolecular nucleophilic attack of the activated oxygen function at a carbonyl ligand and rearrangement, possibly via a carbene intermediate (**C**), yields the reaction product. It should be pointed out that both the product and the proposed reaction pathway are entirely analogous to the results previously established by us for the reaction of similar heterodinuclear complexes with sulfoxides.^[8b, 28] The nature of the functional groups in sulfoxides and cyclopropanones is very similar in that the element–oxygen unit has strong zwitterionic character, the functional group



being additionally polarized and the bond multiplicity reduced.

The conversion leading to **19** appears to be a clear example of cooperative reactivity of the two complementary metal-complex fragments joined in the heterobimetallic complexes. In order to gain additional information regarding the importance of this combination of reactive metal fragments for the observed reaction pathway, 1,2-diphenylcyclopropanone was treated with $K[MCp(CO)_2]$ ($M = Fe, Ru$) only. In both cases, immediate conversion was observed and, after salt metathesis with $[NBu_4]Br$, the salts $[NBu_4][CpM\{C(O)C(Ph)C(Ph)C(O)\}CO]$ ($M = Fe: \mathbf{20a}$, $Ru: \mathbf{20b}$) were isolated (Scheme 12). While the formulation of the reaction



Scheme 12. Reaction of $[MCp(CO)_2]^-$ ($M = Fe, Ru$) with 1,2-diphenylcyclopropanone to yield the metallacyclopenta-2,5-diones.

products was based on the elemental analysis, the infrared spectra of both compounds, **20a** and **20b**, display a single $\nu(CO)$ band at 1883 and 1896 cm^{-1} , respectively, the position of which is characteristic of monoanionic CpM -carbonyl complexes. In the ^{13}C NMR spectrum two low-field resonances are observed at $\delta = 224.7$ (208.5) assigned to the CO ligand and at $\delta = 276.0$ (260.1). Since an unambiguous assignment of the molecular structure of both complexes was not possible based on these data, a single-crystal X-ray structure analysis of compound **20a** was carried out. Two views of its molecular structure are shown in Figure 3; the principal bond lengths and interbond angles are given in the legend.

The metallacyclopenta-2,5-dione ring constitutes the structural centre piece of the organometallic anion. This cyclic unit is not planar but was found to adopt an envelope conformation in which the plane spanned by C(1), C(2), C(3) and C(4) is tilted by 17.6° with respect to the plane defined by C(1), Fe(1) and C(4). The Fe(1)–C(1) and Fe(1)–C(4) bond lengths [1.905(5) and 1.899(6) Å, respectively] lie within the range expected for acyliron units and the C–C bond lengths within the metallacycle are consistent with their formulation as single bonds [C(1)–C(2) 1.524(7), C(1)–C(4) 1.528(7) Å] and a central double bond [C(2)–C(3) 1.344(7) Å].

A very similar reaction product has been reported by Hoffmann and Weiss, who isolated tetracarbonyl-ferra-3-cyclopenten-2,5-dione from the reaction of $[Fe_3(CO)_{12}]$ with acetylene.^[31] Related compounds were also studied by Liebeskind et al. who generated the metallacyclopentene-2,5-

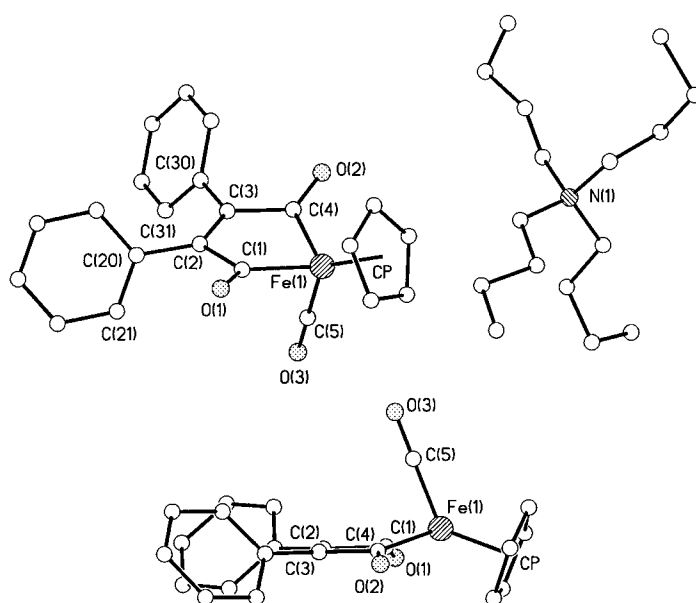


Figure 3. Top: molecular structure of $[Bu_4][CpFe\{C(O)C(Ph)C(Ph)C(O)\}CO]$ (**20a**). Principal bond lengths [Å] and angles [°]: Fe(1)–C(1) 1.905(5), Fe(1)–C(4) 1.899(6), Fe(1)–C(5) 1.718(7), C(1)–C(2) 1.524(7), C(2)–C(3) 1.344(7), C(3)–C(4) 1.528(7), C(1)–O(1) 1.241(6), C(4)–O(2) 1.232(6), C(1)–Fe(1)–C(4) 82.4(2), Fe(1)–C(1)–C(2) 114.4(4), C(1)–C(2)–C(3) 112.1(4), C(2)–C(3)–C(4) 112.6(5), Fe(1)–C(4)–C(3) 114.3(4). Bottom: view parallel to the metallacycle ring planes showing the envelope conformation.

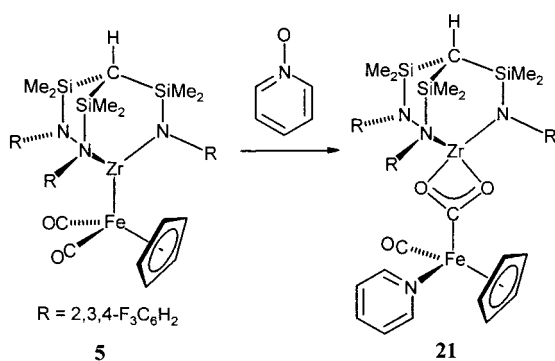
dione units by reaction of cyclobutanediones with low-valent cobalt and rhodium complexes.^[32]

Addition of the chlorozirconium complex **2b** to a solution of **20a** did not convert the anion to the oxygen-transfer product **19**, which resulted from the reaction of the cyclopropanone with the Zr–Fe heterodinuclear complex **5**. Instead, a complicated mixture of products was obtained in which **19** could not be identified even as a minor component. This finding highlights the importance of both the nucleophilic and electrophilic metal centres in the oxygen transfer and conversion of a carbonyl ligand to a bridging CO_2 unit.

Oxygen transfer to CO in reactions of the heterobimetallic complexes with pyridine *N*-oxide and sulfoxides:

Bergman and co-workers recently reported the rapid transfer of oxygen and sulfur from organic molecules to the Zr–Ir bond of $[Cp_2Zr(-N-tBu)IrCp^*]$ to yield products in which the metal–metal bond is cleaved and a bridging oxo or sulfido ligand formed linking the two metal centres.^[18] While no sulfur-transfer reactions involving the Zr–M complexes studied in this work were observed, the heterodinuclear compounds were found to effect oxygen transfer from element oxides to the metal-bonded carbonyl ligands as already indicated by the reaction of the cyclopropanone with **5**. We therefore decided to study the reactions with amine *N*-oxides and sulfoxides.

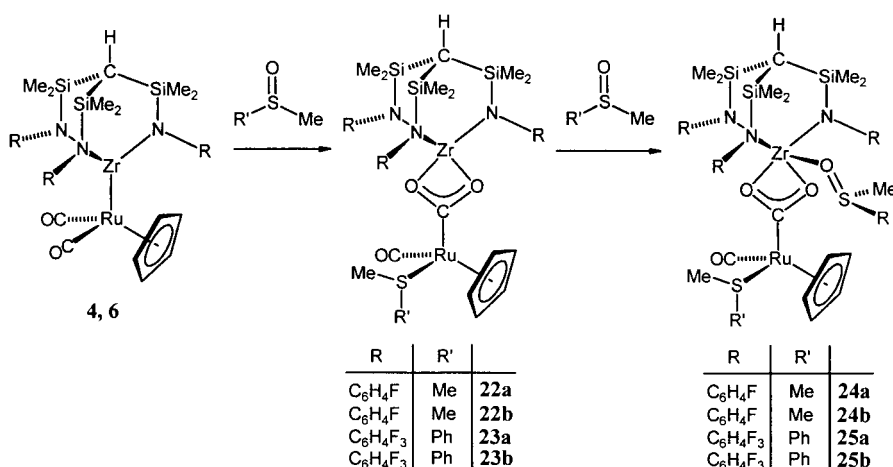
Whereas the reaction of **3–6** with trimethylamine *N*-oxide led to unspecific degradation of the complexes, reaction of **5** with pyridine *N*-oxide yielded the CO_2 -linked complex $[HC\{SiMe_2N(2,3,4-F_3C_6H_2)\}Zr(-O_2C)FeCp(CO)(py)]$ (**21**) (Scheme 13).

Scheme 13. Deoxygenation of pyridine *N*-oxide.

As in the case of **19**, the generation of a chiral iron centre is reflected in the diastereotopic splitting of the SiMe₂ resonances [$\delta(^1\text{H}) = 0.47, 0.54$; $\delta(^{13}\text{C}) = 4.3, 4.7$]. The ¹³C NMR signal of the remaining carbonyl ligand is observed at $\delta = 221.7$, while the linking $\mu\text{-CO}_2$ ligand is characterized by the resonance at $\delta = 250.1$. It is probably owing to the high oxidizing power of the pyridine *N*-oxide that some nonspecific degradation is observed which is manifested in the generation of a small amount of [Fe₂Cp₂(CO)₄].

We have very recently reported oxygen-atom transfer from sulfoxides to carbonyl ligands in Zr–Ru heterodinuclear complexes that are related to **4** and **6**.^[28] Reaction of complexes **4** and **6** with one molar equivalent of Me(R')SO yields the CO₂-linked species [HC{SiMe₂N(R)}Zr(-O₂C)RuCp(CO){S(R')-Me}] (R = 2-FC₆H₄, R' = Me **22a**; R = 2-FC₆H₄, R' = Ph **22b**; R = 2,3,4-F₃C₆H₂, R' = Me **23a**; R = 2,3,4-F₃C₆H₂, R' = Ph **23b**) (Scheme 14). Addition of a second molar equivalent of the sulfoxide yields the Lewis acid–base products species [HC{SiMe₂N(R)}{Me(R)SO- κ O}Zr(-O₂C)RuCp(CO){S(R')-Me}] (**24a/b**, **25a/b**) in which one molecule of sulfoxide is thought to coordinate to the zirconium centre through the oxygen atom. An closely related example of such a species was recently characterized by X-ray crystallography the structure of which could therefore be unambiguously established.^[28]

As in the reaction of **5** with 1,2-diphenylcyclopropenone discussed above, the oxygen transfer from the sulfoxide to the



Scheme 14. Oxygen transfer from sulfoxides to CO within the coordination sphere of Zr–Ru heterodinuclear complexes.

carbonyl ligand, which is converted to the $\mu\text{-CO}_2$ unit, was proved by using ¹³C enriched **6**. In addition we carried out the reaction of **6** with 30% ¹⁷O-enriched methylphenylsulfoxide [$\delta(^{17}\text{O}) = -0.1$, reference: dioxane]. The chemical shift of the product signal of $\delta = 343$ in the labelled complex **23b** is again indicative of an ¹⁷O nucleus in a metallacarboxylato environment.^[30]

Conclusion

The instability of most early–late heterobimetallic complexes that have been synthesized and studied to date has prohibited a systematic study into their reactivity and the testing of the claim of cooperative reactivity. In this study we have shown that the use of amido tripod ligands and thus the integration of the early transition metal centre into a rigid molecular cage, along with the introduction of a partially fluorinated ligand periphery, has allowed the investigation of a wide range of reactions involving the polar metal–metal bonds. These range from simple insertions into the metal–metal bond to cascades of elementary reactions leading to substrate coupling as in the case of the aldol condensation of ketones to atom-transfer reactions, such as those observed in the Cannizzaro disproportionation of aryl aldehydes, and the oxygen transfer involving various element oxides.

In all these cases not only the selectivity of the conversions (as established by monitoring the reactions by NMR spectroscopy) is remarkable but the rapidity with which they occur. Even at very low temperatures aldol coupling or the oxygen transfer to the carbonyl ligands takes place instantaneously and lies outside the regime of conventional kinetic methods.

The role of the early transition metal centre in all these cases appears to be that of polarizing the substrate and thus activating it for nucleophilic attack by the late transition metal complex fragment. The role of the late transition metal fragment is that of a nucleophile in the initial reaction step. Subsequently it may (formally) function as a base, as observed in the aldol chemistry, or as bearer of the oxygen-atom acceptor ligands CO, as found in the reactions with element oxides. Finally, in all the cases we studied, the highly polar metal–metal bond provides the readily and preferentially cleaved interface between the two complementary reactive complex fragments.

Experimental Section

All manipulations were performed under an inert gas atmosphere of dried argon in standard (Schlenk) glassware, which was flame dried with a Bunsen burner prior to use. Solvents were dried according to standard procedures and saturated with Ar. The deuterated solvents used for the NMR spectroscopic measurements were degassed by three successive “freeze–pump–thaw” cycles and dried over 4 Å molecular sieves.

$^1J_{CF} = 246$ Hz, C^4 , $C_6H_2F_3$), 203.3 (br, CO), 237.8 (br, CO_2); 1H ^{17}O NMR (C_6D_6 , 295 K): $\delta = 343.2$ (br, $\Delta\nu_{1/2} = 50$ Hz); 1H ^{29}Si NMR (C_6D_6 , 295 K): $\delta = 0.8$ (s, $SiMe_2$); IR (benzene): $\tilde{\nu}(CO) = 1948$ cm^{-1} ; $C_{39}H_{38}F_9N_3O_3RuSi_2Zr$ (1076.35): calcd C 43.52, H 3.56, N 3.90; found C 42.89, H 3.53, N 4.02.

General Procedure for the preparation of $[HC(SiMe_2N(R))_3(OS(Me)R')Zr(\mu-O_2C)RuCp(CO)(S(Me)R'')]$ (24**, **25**) ($R = 2-FC_6H_4$ or $2,3,4-FC_6H_3$; $R' = Me$ or Ph):** Benzene (15 mL) was added to a solution of **2a** or **2b** (0.6 mmol) and $K[Ru(CO)_2Cp]$ (1.56 mg, 0.6 mmol), and the reaction mixture was placed in an ultrasound bath for 1 h. The reaction mixture was subsequently centrifuged and two equivalents of the sulfoxide were added to the centrifugate. The NMR spectra of the solution indicated a complete and selective conversion of the starting material to the respective products. Upon concentration in vacuo to about 4 mL and storage at $-30^\circ C$ for several days, small amounts of the reaction products precipitated as orange-yellow microcrystalline solids. The low isolated yields are due to the high solubility of the reaction products as well as slow decomposition in solution even at low temperature.

$[HC(SiMe_2N(2-FC_6H_4))_3(OS(Me)_2)Zr(\mu-O_2C)RuCp(CO)(S(Me)_2)]$ (24a**):** Yield: 41%; 1H NMR (C_6D_6 , 295 K): $\delta = -0.12$ (s, $HC(SiMe_2)_3$), 0.51–0.66 (s, $SiMe_2$), 1.51 (s, $(CH_3)_2SO$), 1.89 (s, $(CH_3)_2S$), 4.44 (s, C_5H_5), 6.40–7.47 (m, $2-FC_6H_4$); 1H ^{13}C NMR (C_6D_6 , 295 K): $\delta = 2.50$ (s, $HC(SiMe_2)_3$), 4.33–5.06 (s, $SiMe_2$), 28.09 (s, $(Me)_2$), 37.56 (s, $(OS(Me)_2)$), 86.70 (s, C_5H_5), 207.07 (CO), 227.07 (CO), 115.20 (d, $^2J_{FC} = 12.88$ Hz, C^3 , $2-FC_6H_4$), 120.89, 123.59, 130.04 (C^{4-6} , $2-FC_6H_4$), 142.73 (d, $^2J_{FC} = 14.09$ Hz, C^1 , $2-FC_6H_4$), 158.34 (d, $^1J_{FC} = 240.67$ Hz, C^2 , $2-FC_6H_4$); 1H ^{19}F NMR (C_6D_6 , 295 K): $\delta = -119.86$ ($2-FC_6H_4$); IR (toluene): $\tilde{\nu}(CO) = 1944$ cm^{-1} ; $C_{36}H_{48}F_3N_3O_4RuSi_2Zr$ (984.47): calcd C 43.92, H 4.91, N 4.27; found C 43.68, H 4.63, N 3.97.

$[HC(SiMe_2N(2-FC_6H_4))_3(OS(Me)Ph)Zr(\mu-O_2C)RuCp(CO)(S(Me)Ph)]$ (24b**):** Yield: 37%; 1H NMR (C_6D_6 , 295 K): $\delta = -0.08$ (s, $1H$, $HC(SiMe_2)_3$), 0.55, 0.63 (s, $18H$, $SiMe_2$), 1.98 (s, $3H$, $CH_3SOC_6H_5$), 2.42 (s, $3H$, $CH_3SC_6H_5$), 4.36 (s, $5H$, C_5H_5), 6.41–7.36 (m, $22H$, $C_6H_2F_3$, C_6H_5SMe and $C_6H_5SOCH_3$); 1H ^{13}C NMR (C_6D_6 , 295 K): $\delta = 2.4$ (s, $HC(SiCH_3)_2$), 4.4, 4.7 (s, $SiMe_2$), 30.2 (s, $H_3CSC_6H_5$), 42.5 (br, $H_3CSOC_6H_5$), 87.1 (s, C_5H_5), 115.3 (d, $^2J_{FC} = 22$ Hz, C^3 , C_6H_4FN), 124.0 (s, $CH_3SC_6H_5$), 129.5 (s, $CH_3SOC_6H_5$), 130.2 (s, $CH_3SOC_6H_5$), 130.8 (s, $CH_3SOC_6H_5$), 141.8 (s, $CH_3SC_6H_5$), 142.0 (s, $CH_3SC_6H_5$), 142.1 (s, $CH_3SC_6H_5$), 158.2 (d, $^1J_{FC} = 242$ Hz, C^2 , C_6H_4FN), 206.5 (s, CO), 227.0 (s, CO_2); 1H ^{19}F NMR ($[D_8]toluene$, 295 K): $\delta = -117.9$ (s, F^2); 1H ^{29}Si NMR ($[D_8]toluene$, 295 K): $\delta = 0.3$ (s, $SiCH_3$); IR (toluene): $\tilde{\nu}(CO) = 1961$ cm^{-1} ; $C_{46}H_{52}F_3N_3O_4RuSi_2Zr$ (1108.61): calcd C 49.84, H 4.73, N 3.79; found C 49.48, H 4.59, N 3.66.

$[HC(SiMe_2N(2,3,4-F_3C_6H_2))_3(OS(Me)_2)Zr(\mu-O_2C)RuCp(CO)(S(Me)_2)]$ (25a**):** Yield: 42%; 1H NMR (C_6D_6 , 295 K): $\delta = -0.30$ (s, $HC(SiMe_2)_3$), 0.38 (s, $SiMe_2$), 1.60 (s, $(CH_3)_2S$), 4.37 (s, C_5H_5), 6.40–6.60 (m, $2,3,4-F_3C_6H_2$); 1H ^{13}C NMR (C_6D_6 , 295 K): $\delta = 4.76$ (s, $HC(SiMe_2)_3$), 4.20 (s, $SiMe_2$), 28.0 (s, $(Me)_2$), 86.65 (s, C_5H_5), 200.08 (CO), 235.35 (CO_2), 110.48 (d, $^2J_{FC} = 16.34$ Hz, C^5 , $2,3,4-F_3C_6H_2$), 120.39 (C^6 , $2,3,4-F_3C_6H_2$), 138.10 (d, $^2J_{FC} = 15.0$ Hz, C^1 , $2,3,4-F_3C_6H_2$), 140.89 (dt, $^1J_{FC} = 248.63$ Hz, $^2J_{FC} = 16.10$ Hz, C^3 , $2,3,4-F_3C_6H_2$), 146.16 (dd, $^1J_{FC} = 241.8$ Hz, $^2J_{FC} = 9.8$ Hz, C^4 , $2,3,4-F_3C_6H_2$), 146.78 (dd, $^1J_{FC} = 241.8$ Hz, $^2J_{FC} = 7.84$ Hz, C^2 , $2,3,4-F_3C_6H_2$); 1H ^{19}F NMR (C_6D_6 , 295 K): $\delta = -161.32$ (t, $J_{FF} = 22.4$ Hz, F_2), -146.13 (d, $J_{FF} = 22.6$ Hz, F_4), -145.75 (d, $J_{FF} = 22.2$ Hz, F_2); 1H ^{29}Si NMR (C_6D_6 , 295 K): $\delta = -10.66$; IR (toluene): $\tilde{\nu}(CO) = 1930$ cm^{-1} ; $C_{36}H_{42}F_9N_3O_3RuSi_2Zr$ (1092.42): calcd C 39.58, H 3.88, N 3.85; found C 39.78, H 3.67, N 3.94.

$[HC(SiMe_2N(2,3,4-F_3C_6H_2))_3(OS(Me)Ph)Zr(\mu-O_2C)RuCp(CO)(S(Me)Ph)]$ (25b**):** Yield: 31%; 1H NMR (C_6D_6 , 295 K): $\delta = -0.22$ (s, $1H$, $HC(SiMe_2)_3$), 0.49, 0.52 (s, $18H$, $SiMe_2$), 1.89 (s, $3H$, $CH_3SOC_6H_5$), 2.38 (s, $3H$, $CH_3SC_6H_5$), 4.34 (s, $5H$, C_5H_5), 6.41–7.36 (m, $16H$, $C_6H_2F_3$, C_6H_5SMe and $C_6H_5SOCH_3$); 1H ^{13}C NMR (C_6D_6 , 295 K): $\delta = 2.4$ (s, $HC(SiCH_3)_2$), 4.5, 4.7 (s, $SiMe_2$), 30.1 (s, $H_3CSC_6H_5$), 41.1 (br, $H_3CSOC_6H_5$), 87.7 (s, C_5H_5), 110.0 (dd, $^2J_{FC} = 17$ Hz, $^3J_{CF} = 4$ Hz, C^1 , $C_6H_2F_3$), 122.6 (d, $^3J_{CF} = 5$ Hz, C^6 , $C_6H_2F_3$), 124.3 (s, $C_6H_5SOCH_3/C_6H_5SCH_3$), 125.3 (s, $C_6H_5SOCH_3/C_6H_5SCH_3$), 127.1 (s, $C_6H_5SOCH_3/C_6H_5SCH_3$), 129.3 (s, $C_6H_5SOCH_3/C_6H_5SCH_3$), 129.6 (s, $C_6H_5SOCH_3/C_6H_5SCH_3$), 129.9 (s, $C_6H_5SOCH_3/C_6H_5SCH_3$), 131.8 (s, $C_6H_5SOCH_3/C_6H_5SCH_3$), 139.4 (dd, $^2J_{FC} = 12$ Hz, $^3J_{FC} = 4$ Hz, C^5 , $C_6H_2F_3$), 141.2 (dt, $^1J_{FC} = 247$ Hz, $^2J_{FC} = 17$ Hz, C^3 , $C_6H_2F_3$), 141.4 (s, $C_6H_5SOCH_3/C_6H_5SCH_3$), 146.3 (dd, $^1J_{FC} = 232$ Hz, $^2J_{FC} = 8$ Hz, C^2 , $C_6H_2F_3$), 147.1 (ddd, $^1J_{FC} = 243$ Hz, $^2J_{FC} = 8$ Hz, $^3J_{CF} = 4$ Hz, C^4 , $C_6H_2F_3$), 206.3 (s, CO), 228.7 (s, CO_2); 1H ^{17}O NMR (C_6D_6 , 27.1 MHz): $\delta = 2.0$ (br, $\Delta\nu_{1/2} = 300$ Hz), 343.2 (br, $\Delta\nu_{1/2} = 50$ Hz); 1H ^{19}F

NMR (C_6D_6 , 376.4 MHz): $\delta = -161.2$ (t, $^3J_{FF} = 22$ Hz, F^3), -145.8 (d, $^3J_{FF} = 21$ Hz, F^4), -140.9 (d, $^3J_{FF} = 22$ Hz, F^2); 1H ^{29}Si NMR (C_6D_6 , 79.5 MHz): $\delta = 0.8$ (s, $SiCH_3$); IR (benzene): $\tilde{\nu}(CO) = 1942$ cm^{-1} ; $C_{46}H_{46}F_9N_3O_4RuSi_2Zr$ (1216.56): calcd C 45.42, H 3.81, N 3.45; found C 45.28, H 3.97, N 3.24.

Synthesis of ^{17}O -enriched methylphenylsulfoxide: Thioanisol (0.94 g, 7.757 mmol) was dissolved in dichloromethane (2 mL) and pyridine (0.5 mL). A mixture of $H_2^{17}O$ (0.15 mL, 35% enriched) and pyridine (0.5 mL) were added to the stirred solution followed by bromine (1.33 g, 8.32 mmol). After having stirred for 1 h the solvents were removed in vacuo and the residue was extracted with benzene (4×15 mL). The benzene extracts were combined and the solvent evaporated in vacuo. The residue was then redissolved in diethyl ether (1 mL) and the sulfoxide was precipitated by addition of pentane (10 mL) to this solution. After decanting, the crude ^{17}O -enriched sulfoxide was purified by Kugelrohr distillation. Yield 0.20 g (1.42 mmol, 19%). The simulation of the EI mass spectrum of the material established an ^{17}O -enrichment of about 30%; 1H NMR ($CDCl_3$): $\delta = 2.68$ (s, $3H$, CH_3), 7.46–7.63 (m, $5H$, C_6H_5); 1H ^{13}C NMR ($CDCl_3$): $\delta = 43.9$ (s, CH_3), 123.5 (s, $C^{2,6}$, C_6H_5), 129.3 (s, $C^{3,5}$, C_6H_5), 131.0 (s, C^4 , C_6H_5), 145.7 (s, C^1 , C_6H_5); 1H ^{17}O NMR ($CDCl_3$): $\delta = 0.1$ (br, $\Delta\nu_{1/2} = 270$ Hz).

X-ray crystallographic studies of **2b, **9a**, **12** and **20a**.**

Data collection for **2b, **9a**, **12** and **20a**:** Crystals of **2b**, **9a**, **12** and **20a** were mounted on quartz fibres in Lindemann capillaries under argon and in an inert oil. X-ray intensity data were collected with graphite-monochromated radiation on four-circle diffractometers (Siemens P4 for **2b** and **9a**, Phillips PW1100 for **12**, Enraf-Nonius CAD-4 for **20a**). Details of data collection, refinement and crystal data are listed in Table 3. Lorentz polarisation and absorption corrections were applied to the data of all the compounds.

Structure solution and refinement for **2b, **9a**, **12** and **20a**:** For compounds **2b**, **9a**, and **20a** the positions of most of the non-hydrogen atoms were located by direct methods and for **12** the metal atoms were located from a Patterson synthesis; for all structures the remaining non-hydrogen atoms were revealed from subsequent difference-Fourier syntheses. All the structures showed some disorder, which accounts for the relatively poor diffraction at high angle. In **2b**, two conformations of the ethyl groups of the two Et_2O ligands were disordered throughout the crystal; each carbon atom was resolved into two components of 0.5 site occupancy. In both insertion products **9a** and **12**, marked anisotropy of the displacement parameters of the phenyl carbon atoms provided evidence of some unresolved disorder; in **9a** two pairs of maxima of electron density at bonding distance from the *ortho*-carbon atoms C(12), C(16) and C(22), C(26) were each interpreted as F-atoms of site of occupancies 0.90:0.10 corresponding to orientations of the phenyl rings, related by a rotation of 180° . A similar situation arose for the fluorine atoms F(1) and F(2) of **12**; here the two components for each atom were assigned site occupancies of 0.75:0.25 for F(1) and 0.5:0.5 for F(2). A second disorder was observed in the structure of **12**; two maxima were identified for each atom of the $SiMe_2$ groups corresponding to a random distribution of two molecules with opposite "twist" of the tripod framework in equivalent sites throughout the crystal; the component silicon and carbon atoms were assigned site occupancies of 0.75 and 0.25, and the carbon atoms of the minor component were not refined. The extensive disorder in this structure results in relatively high esd 's for the metric parameters, but the overall structure of this new insertion product is well established. In compound **20a** two conformations of the $[N(nBu)_4]^+$ cation were randomly distributed throughout the crystal; each carbon atom of the *n*-butyl groups of this counterion was resolved into two components of site occupancies 0.667 and 0.333. For the structure of **12** refinement was based on F^{136a} and for the three other structures refinement was based on $F^{2,136b}$. Phenyl rings were constrained to idealised geometry ($C-H = 1.390$ Å). The hydrogen atoms of the cyclopentadienyl rings in **9a**, **12**, and **20a** and of the phenyl rings in **20a** were directly located from Fourier difference syntheses and were included in structure factor calculation, but were not refined. All other hydrogen atoms (except those of the minor component of the $SiMe_2$ disorder in **12**) were placed in calculated positions. Isotropic displacement parameters were assigned to all hydrogen atoms, with a fixed at a value of 0.12 Å² in **12**, and in the other three structures set equal to $1.2 U_{eq}$ of the parent carbon atoms for the phenyl, cyclopentadienyl and methylene groups and $1.5 U_{eq}$ for the methyl groups. Semi-empirical absorption corrections^[36b] using ψ -scans were applied to the data of **9a**, **12** and **20a**, and

Table 3. Crystal data and structure refinement for complexes **2b**, **9a**, **12** and **20a**.

	2b	9a	12	20a
formula	C ₃₃ H ₄₅ Cl ₂ F ₉ N ₅ O ₂ Si ₃ Zr	C ₃₃ H ₃₆ F ₃ FeN ₅ O ₂ S ₂ Si ₃ Zr	C ₃₀ H ₄₁ N ₄ O ₂ F ₃ Si ₃ SFeZr	C ₄₄ H ₅₇ FeNO ₃
<i>M</i> _r	940.05	859.11	918.17	703.76
crystal system	monoclinic	triclinic	monoclinic	triclinic
space group	<i>P</i> 2 ₁ / <i>c</i>	<i>P</i> 1	<i>P</i> 2 ₁ / <i>n</i>	<i>P</i> 1
<i>a</i> [Å]	18.150(4)	10.293(4)	19.388(3)	10.6664(10)
<i>b</i> [Å]	18.118(6)	12.538(3)	17.358(3)	10.9162(10)
<i>c</i> [Å]	13.422(3)	16.294(5)	12.642(2)	19.6979(10)
<i>α</i> [°]	–	97.76(2)	–	75.493(10)
<i>β</i> [°]	95.15(2)	90.804(16)	90.72(3)	89.953(1)
<i>γ</i> [°]	–	111.53(3)	–	63.082(1)
<i>V</i> [Å ³]	4396(2)	1933.5(10)	4254(2)	1962.9(3)
<i>Z</i>	4	2	4	2
<i>ρ</i> _{calcd} [g cm ⁻³]	1.420	1.476	1.434	1.191
radiation (λ [Å])	MoK _α (0.71073)	MoK _α (0.71073)	MoK _α (0.71069)	MoK _α (0.71073)
<i>μ</i> [mm ⁻¹]	0.524	0.893	0.730	0.424
<i>F</i> (000)	1920	876	1880	756
crystal size [mm]	0.58 × 0.32 × 0.30	0.30 × 0.16 × 0.10	0.35 × 0.22 × 0.20	0.60 × 0.20 × 0.10
<i>θ</i> range [°]	1.89–21.00	1.77–21.00	3.00–21.00	2.14–22.00
index range	–18 ≤ <i>h</i> ≤ 18 –18 ≤ <i>k</i> ≤ 1 –1 ≤ <i>l</i> ≤ 13	–1 ≤ <i>h</i> ≤ 10 –12 ≤ <i>k</i> ≤ 12 –16 ≤ <i>l</i> ≤ 16	–19 ≤ <i>h</i> ≤ 19 0 ≤ <i>k</i> ≤ 17 0 ≤ <i>l</i> ≤ 11	–2 ≤ <i>h</i> ≤ 11 –11 ≤ <i>k</i> ≤ 11 –20 ≤ <i>l</i> ≤ 20
reflections collected	5906	5059	4622	5811
independent reflections (<i>R</i> _{int})	4708 (0.0773)	4163 (0.0932)	1874 [<i>I</i> /σ(<i>I</i>) > 3]	4822 (0.0400)
max/min transmission	0.7740/0.3559	0.9902/0.8930	1.0000/0.7934	1.0000/0.8167
data/restraints/parameters	4708/37/428	4163/35/404	1874/12/267	4822/360/556
<i>S</i> on <i>F</i> ²	0.964	0.927	–	1.053
final <i>R</i> indices ^[a]				
[<i>I</i> > 2σ(<i>I</i>)]	<i>R</i> ₁ = 0.0767, <i>wR</i> ₂ = 0.1756	<i>R</i> ₁ = 0.0789, <i>wR</i> ₂ = 0.0679	<i>R</i> = 0.0654, <i>R</i> ' = 0.0657 ^[b]	<i>R</i> ₁ = 0.0727, <i>wR</i> ₂ = 0.1743
(all data)	<i>R</i> ₁ = 0.1552, <i>wR</i> ₂ = 0.2044	<i>R</i> ₁ = 0.2017, <i>wR</i> ₂ = 0.0826	–	<i>R</i> ₁ = 0.1157, <i>wR</i> ₂ = 0.1965
weights a, b ^[a]	0.1155, 0.0000	0.0054, 0.0000	^[b]	0.1074, 0.9485
max/min Δ <i>ρ</i> [e Å ⁻³]	0.634/–0.461	0.427/–0.454	0.525/–0.501	0.353/–0.342

[a] $S = [\sum w(F_o^2 - F_c^2)^2 / (n - p)]^{1/2}$, in which *n* = number of reflections and *p* = total number of parameters, $R_1 = \sum ||F_o| - |F_c|| / \sum |F_o|$, $R_2 = \sum [w(F_o^2 - F_c^2)^2] / \sum [w(F_o^2)^2]^{1/2}$, $w^{-1} = [\sigma^2(F_o)^2 + (aP)^2 + bP]$, $P = [\max(F_o^2, 0) + 2(F_c^2)]/3$.

[b] For **12**: weights of $1/s^2(F)$ were applied; [*I*/σ(*I*) > 3] $R = \sum(\Delta F) / \sum(F_o)$; $R' = [\sum(\Delta F)^2 / \sum w(F_o)^2]^{1/2}$.

after initial refinement with isotropic displacement parameters empirical absorption corrections^[37] were applied to the data of **2b**. Chemically equivalent bond lengths within the tripod frameworks of **2b**, **9a**, and **12**, and those involving the components of disordered atoms in all structures, were constrained to be equal within an esd of 0.02 Å. All full-occupancy non-hydrogen atoms (except the carbon atoms of **12**), and the atoms of 0.667 occupancy in **20a**, were assigned anisotropic displacement parameters in the final cycles of full-matrix least-squares refinement; those of the benzene solvate in **20a** were constrained to be approximately equal. Crystallographic data (excluding structure factors) for the structures reported in this paper have been deposited with the Cambridge Crystallographic Data Centre as supplementary publication no. CCDC-135460 **2b**, CCDC-135461 **9a**, CCDC-135462 **12** and CCDC-135463 **20a**. Copies of the data can be obtained free of charge on application to CCDC, 12 Union Road, Cambridge CB2 1EZ, UK (fax: (+44) 1223-336-033; e-mail: deposit@ccdc.cam.ac.uk).

Acknowledgements

We thank the Deutsche Forschungsgemeinschaft, the European Union (TMR program, network MECATSYN), the Fonds der Chemischen Industrie, the DAAD and the British Council (ARC 313 grant to L.H.G and M.McP.) for financial support and Degussa AG as well as Wacker Chemie AG for generous gifts of basic chemicals.

[1] a) D. A. Roberts, G. L. Geoffroy, in *Comprehensive Organometallic Chemistry Vol. 6* (Eds.: G. Wilkinson, F. A. G. Stone, E. W. Abel), Pergamon, **1982**, p. 763; b) P. Braunstein, J. Rose, in *Stereochemistry of Organometallic and Inorganic Compounds Vol. 3* (Ed.: I Bernal), Elsevier, Amsterdam, **1989**, p. 3.

- [2] See for example: a) G. S. Ferguson, P. T. Wolczanski, L. Parkanyi, M. Zonneville, *Organometallics* **1988**, *7*, 1967; b) F. Ozawa, J. W. Park, P. B. Mackenzie, W. P. Schaefer, L. M. Henling, R. H. Grubbs, *J. Am. Chem. Soc.* **1989**, *111*, 1319; c) A. M. Baranger, R. G. Bergman, *J. Am. Chem. Soc.* **1994**, *116*, 3822.
- [3] C. P. Casey, *J. Organomet. Chem.* **1990**, *400*, 205.
- [4] a) C. P. Casey, R. F. Jordan, A. L. Rheingold, *J. Am. Chem. Soc.* **1983**, *105*, 665; b) C. P. Casey, R. F. Jordan, A. L. Rheingold, *Organometallics* **1984**, *3*, 504; c) C. P. Casey, R. E. Palermo, R. F. Jordan, *J. Am. Chem. Soc.* **1985**, *107*, 4597; d) C. P. Casey, R. E. Palermo, *J. Am. Chem. Soc.* **1986**, *108*, 549; e) W. S. Sartain, J. P. Selegue, *J. Am. Chem. Soc.* **1985**, *107*, 5818; f) W. S. Sartain, J. P. Selegue, *Organometallics* **1987**, *6*, 1812; g) W. S. Sartain, J. P. Selegue, *Organometallics* **1989**, *8*, 2153; h) D. Selent, R. Beckhaus, J. Pickardt, *Organometallics* **1993**, *12*, 2857.
- [5] A. M. Baranger, T. A. Hanna, R. G. Bergman, *J. Am. Chem. Soc.* **1995**, *117*, 10041.
- [6] M. Schubart, G. Mitchell, L. H. Gade, I. J. Scowen, M. McPartlin, *Chem. Commun.* **1999**, 233.
- [7] a) S. Friedrich, H. Memmler, L. H. Gade, W.-S. Li, M. McPartlin, *Angew. Chem.* **1994**, *106*, 705; *Angew. Chem. Int. Ed. Engl.* **1994**, *33*, 676; b) S. Friedrich, H. Memmler, L. H. Gade, W.-S. Li, I. J. Scowen, M. McPartlin, C. E. Housecroft, *Inorg. Chem.* **1996**, *35*, 2433.
- [8] a) B. Findeis, M. Schubart, C. Platzek, L. H. Gade, I. J. Scowen, M. McPartlin, *Chem. Commun.* **1996**, 219; b) L. H. Gade, M. Schubart, B. Findeis, S. Fabre, I. Bezougli, M. Lutz, I. J. Scowen, M. McPartlin, *Inorg. Chem.* **1999**, *38*, 5282.
- [9] a) S. Friedrich, L. H. Gade, I. J. Scowen, M. McPartlin, *Angew. Chem.* **1996**, *108*, 1440; *Angew. Chem. Int. Ed. Engl.* **1996**, *35*, 1338; b) S. Friedrich, L. H. Gade, I. J. Scowen, M. McPartlin, *Organometallics* **1995**, *14*, 5344; c) L. H. Gade, S. Friedrich, D. J. M. Trösch, I. J. Scowen, M. McPartlin, *Inorg. Chem.* **1999**, *38*, 5295.

- [10] G. Jansen, M. Schubart, B. Findeis, L. H. Gade, I. J. Scowen, M. McPartlin, *J. Am. Chem. Soc.* **1998**, *120*, 7239.
- [11] H. Memmler, U. Kauper, L. H. Gade, I. J. Scowen, M. McPartlin, *Chem. Commun.* **1996**, 1751.
- [12] A. Schneider, L. H. Gade, M. Breuning, G. Bringmann, I. J. Scowen, M. McPartlin, *Organometallics*, **1998**, *17*, 1643.
- [13] H. Memmler, K. Walsh, L. H. Gade, J. W. Lauher, *Inorg. Chem.* **1995**, *34*, 4062.
- [14] B. Findeis, M. Schubart, L. H. Gade, I. Scowen, M. McPartlin, *J. Chem. Soc. Dalton Trans.* **1996**, 125.
- [15] a) M. Kol, R. R. Schrock, R. Kempe, W. M. Davis, *J. Am. Chem. Soc.* **1994**, *116*, 4382; b) B. Neuner, R. R. Schrock, *Organometallics* **1996**, *15*, 5; c) R. R. Schrock, C. C. Cummins, T. Wilhelm, S. Lin, S. M. Reid, M. Kol, W. M. Davis, *Organometallics* **1996**, *15*, 1470; d) K. Nomura, R. R. Schrock, W. M. Davis, *Inorg. Chem.* **1996**, *35*, 3695; e) C. Rosenberger, R. R. Schrock, W. M. Davis, *Inorg. Chem.* **1997**, *36*, 123.
- [16] Zr–F distances in “simple” zirconium fluorides or fluorozirconium complexes lie in the range between 1.98 and 2.17 Å: a) D. R. Sears, J. H. Burns, *J. Chem. Phys.* **1964**, *41*, 3478; b) G. Brunton, *Acta Crystallogr. Sect. B* **1969**, *25*, 2164; c) J. Fischer, R. Weiss, *Acta Crystallogr. Sect. B* **1973**, *B29*, 1955; d) M. A. Bush, G. A. Sim, *J. Chem. Soc. A* **1971**, 2225.
- [17] J. R. Pinkes, B. D. Steffey, J. C. Vites, A. R. Cutler, *Organometallics* **1994**, *13*, 21.
- [18] T. A. Hanna, A. M. Baranger, R. G. Bergman, *J. Am. Chem. Soc.* **1995**, *117*, 665.
- [19] See for example: a) S. Gambarotta, M. B. Fiallo, C. Floriani, A. Chiesi-Villa, C. Guastini, *Inorg. Chem.* **1984**, *23*, 3532; b) M. G. B. Drew, J. D. Wilkins, *J. Chem. Soc., Dalton Trans.* **1974**, 198.
- [20] a) M. Pankowski, M. Bigorn, *J. Organomet. Chem.* **1976**, *110*, 331; b) H. Felkin, B. Meunier, C. Pascard, T. Prange, *J. Organomet. Chem.* **1977**, *135*, 361.
- [21] J. March, *Advanced Organic Chemistry*, Wiley, New York, **1992**, p. 1234.
- [22] H. C. Brown, B. C. Subba Rao, *J. Am. Chem. Soc.* **1958**, *80*, 5377.
- [23] A. Schneider, Diplomarbeit, Universität Würzburg, **1996**.
- [24] a) E. J. Kuhlmann, J. J. Alexander, *Inorg. Chim. Acta* **1979**, *34*, L193; b) H. Felkin, B. Meunier, C. Pascard, T. Prange, *J. Organomet. Chem.* **1977**, *135*, 361.
- [25] M. Brookhart, W. B. Studabaker, G. R. Husk, *Organometallics* **1987**, *6*, 1141.
- [26] a) C. P. Casey, W. H. Miles, H. Tukada, *J. Am. Chem. Soc.* **1985**, *107*, 2924; b) M. Akita, T. Kawakara, Y. Moro-oka, *J. Chem. Soc. Chem. Commun.* **1987**, 1356.
- [27] A. Maple, K. Allerhand, *J. Org. Chem.* **1985**, *50*, 4414.
- [28] S. Fabre, B. Findeis, D. J. M. Trösch, L. H. Gade, I. J. Scowen, M. McPartlin, *Chem. Commun.* **1999**, 577.
- [29] a) H. O. Kalinowski, S. Berger, S. Braun, *¹⁷O- und ²⁹Si-NMR-Spektroskopie*, Thieme, Stuttgart, 1984; b) I. P. Gerotheranassis, J. Lauterwein, *Mag. Res. Chem.* **1986**, *24*, 1034.
- [30] A. Lycka, J. Holecek, *J. Organomet. Chem.* **1985**, *265*, 273.
- [31] K. Hoffmann, E. Weiss, *J. Organomet. Chem.* **1977**, *128*, 399.
- [32] a) M. A. Huffman, L. S. Liebeskind, W. T. Pennington, Jr., *Organometallics* **1990**, *9*, 2194; b) S. H. Cho, K. R. Wirtz, L. S. Liebeskind, *Organometallics* **1990**, *9*, 3067.
- [33] a) S. W. Tobey, R. West, *J. Am. Chem. Soc.* **1964**, *86*, 1459; b) H. Yoshita, M. Aoyama, F. Utsumi, T. Ogata, K. Matsumoto, *Bull. Chem. Soc. Jpn.* **1991**, *64*, 3476.
- [34] D. J. Darensbourg, R. L. Gray, M. Pala, *Organometallics* **1984**, *3*, 1928.
- [35] M. I. Bruce, C. M. Jensen, N. L. Jones, *Inorg. Synth.* **1990**, *28*, 216.
- [36] a) G. M. Sheldrick, *SHELX-76, Program for Crystal Structure Determination*, University of Cambridge, **1976**; b) *SHELXTL (PC version 5.03)*, Siemens Analytical Instruments, Madison, WI, **1994**.
- [37] N. Walker, D. Stuart, *Acta Crystallogr. Sect. A.* **1983**, *39*, 158.

Received: August 2, 1999 [F1949]